International Tables for Crystallography (2006). Vol. C, Section 2.2.1, pp. 26–29.

2.2. Single-crystal X-ray techniques

By J. R. Helliwell

In Chapter 2.1 *Classification of experimental techniques* there are given the various common approaches to the recording of X-ray crystallographic data, in different geometries, for crystal structure analysis. These are:

(*a*) Laue geometry;
(*b*) monochromatic still exposure;
(*c*) rotation/oscillation geometry;
(*d*) Weissenberg geometry;
(*e*) precession geometry;
(*f*) diffractometry.

The reasons for the choice of order are as follows. Laue geometry is dealt with first because it was historically the first to be used (Friedrich, Knipping & von Laue, 1912). In addition, the first step that should be carried out with a new crystal, at least of a small molecule, is to take a Laue photograph to make the first assessment of crystal quality. For macromolecules, the monochromatic still serves the same purpose. From consideration of the monochromatic still geometry, we can then describe the cases of single-axis rotation (rotation/oscillation method), single-axis rotation coupled with detector translation (Weissenberg method), crystal and detector precession (precession method), and finally three-axis goniostat and rotatable detector or area detector (diffractometry).

Method (*a*) uses a polychromatic beam of broad wavelength bandpass (*e.g.* $0.2 \leq \lambda \leq 2.5$ Å); if the bandwidth is restricted (*e.g.* to $\delta\lambda/\lambda = 0.2$), then it is sometimes referred to as narrow-bandpass Laue geometry. The remaining methods (*b*)–(*f*) use a monochromatic beam.

There are textbooks that concentrate on almost every geometry. References to these books are given in the respective sections in the following pages. However, in addition, there are several books that contain details of diffraction geometry. Blundell & Johnson (1976) describe the use of the various diffraction geometries with the examples taken from protein crystallography. There is an extensive discussion and many practical details to be found in the textbooks of Stout & Jensen (1968), Woolfson (1970, 1997), Glusker & Trueblood (1971, 1985), Vainshtein (1981), and McKie & McKie (1986), for example. A collection of early papers on the diffraction of X-rays by crystals involving, *inter alia*, experimental techniques and diffraction geometry, can be found in Bijvoet, Burgers & Hägg (1969, 1972). A collection of papers on, primarily, protein and virus crystal data collection *via* the rotation-film method and diffractometry can be found in Wyckoff, Hirs & Timasheff (1985). Synchrotron instrumentation, methods, and applications are dealt with in the books of Helliwell (1992) and Coppens (1992).

Quantitative X-ray crystal structure analysis usually involves methods (*c*), (*d*), and (*f*), although (*e*) has certainly been used. Electronic area detectors or image plates are extensively used now in all methods.

Traditionally, Laue photography has been used for crystal orientation, crystal symmetry, and mosaicity tests. Rapid recording of Laue patterns using synchrotron radiation, especially with protein crystals or with small crystals of small molecules, has led to an interest in the use of Laue geometry for quantitative structure analysis. Various fundamental objections made, especially by W. L. Bragg, to the use of Laue geometry have been shown not to be limiting.

The monochromatic still photograph is used for orientation setting and mosaicity tests, for protein or virus crystallography, and computer refinement of crystal orientation following initial crystal setting.

Precession photography allows the isolation of a specific zone or plane of reflections for which indexing can be performed by inspection, and systematic absences and symmetry are explored. From this, space-group assignment is made. The use of precession photography is usually avoided in small-molecule crystallography where auto-indexing methods are employed on a single-crystal diffractometer. In such a situation, the burden of data collection is not huge and symmetry elements can be determined after data collection. This is also now carried out on electronic area detectors in conjunction with auto-indexing principally at present for macromolecular crystallography but also for chemical crystallography.

In the following sections, the geometry of each method is dealt with in an idealized form. The practical realization of each geometry is then dealt with, including the geometric distortions introduced in the image by electronic area detectors. A separate section deals with the common means for beam conditioning, namely mirrors, monochromators, and filters. Sufficient detail is given to establish the magnitude of the wavelength range, spectral spreads, beam divergence and convergence angles, and detector effects. These values can then be utilized along with the formulae given for the calculation of spot bandwidth, spot size, and angular reflecting range.

2.2.1. Laue geometry

The main book dealing with Laue geometry is Amorós, Buerger & Amorós (1975). This should be used in conjunction with Henry, Lipson & Wooster (1951), or McKie & McKie (1986); see also Helliwell (1992, chapter 7). There is a synergy between synchrotron and neutron Laue diffraction developments (see Helliewell & Wilkinson, 1994).

2.2.1.1. *General*

The single crystal is bathed in a polychromatic beam of X-rays containing wavelengths between $\lambda_{\min}$ and $\lambda_{\max}$. A particular crystal plane will pick out a general wavelength λ for which constructive interference occurs and reflect according to Bragg's law

$$\lambda = 2d \sin\theta, \qquad (2.2.1.1)$$

where d is the interplanar spacing and θ is the angle of reflection. A sphere drawn with radius $1/\lambda$ and with the beam direction as diameter, passing through the origin of the reciprocal lattice (the point O in Fig. 2.2.1.1), will yield a reflection in the direction drawn from the centre of the sphere and out through the reciprocal-lattice point (relp) provided the relp in question lies on the surface of the sphere. This sphere is known as the Ewald sphere. Fig. 2.2.1.1 shows the Laue geometry, in which there exists a nest of Ewald spheres of radii between $1/\lambda_{\max}$ and $1/\lambda_{\min}$. An alternative convention is feasible whereby only a single Ewald sphere is drawn of radius 1 reciprocal-lattice unit (r.l.u.). Then each relp is no longer a point but a streak between $\lambda_{\min}/d$ and $\lambda_{\max}/d$ from the origin of reciprocal space (see McKie & McKie, 1986, p. 297). In the following discussions on the Laue approach, this notation is not followed. We use the nest of Ewald spheres of varying radii instead.

Any relp (*hkl*) lying in the region of reciprocal space between the $1/\lambda_{max}$ and $1/\lambda_{min}$ Ewald spheres and the resolution sphere $1/d_{min}$ will diffract (the shaded area in Fig. 2.2.1.1). This region of reciprocal space is referred to as the accessible or stimulated region. Fig. 2.2.1.2 shows a predicted Laue pattern from a well aligned protein crystal. For a description of the indexing of a Laue photograph, see Bragg (1928, pp. 28, 29).

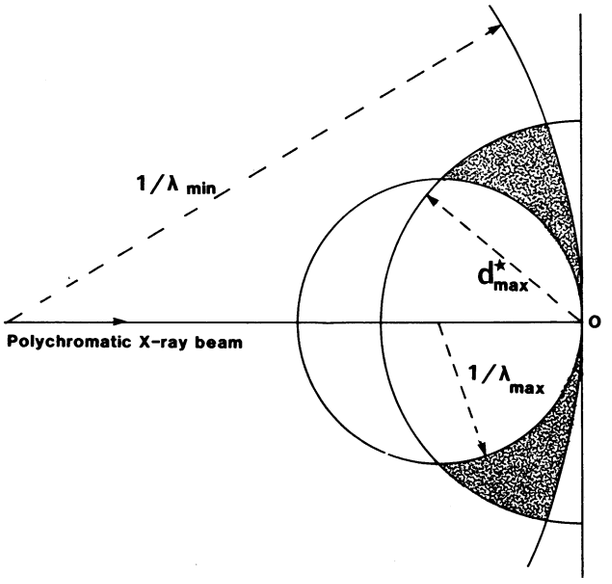

Fig. 2.2.1.1. Laue geometry. A polychromatic beam containing wavelengths λ_{min} to λ_{max} impinges on the crystal sample. The resolution sphere of radius $d^*_{max} = 1/d_{min}$ is drawn centred at O, the origin of reciprocal space. Any reciprocal-lattice point falling in the shaded region is stimulated. In this diagram, the radius of each Ewald sphere uses the convention $1/\lambda$.

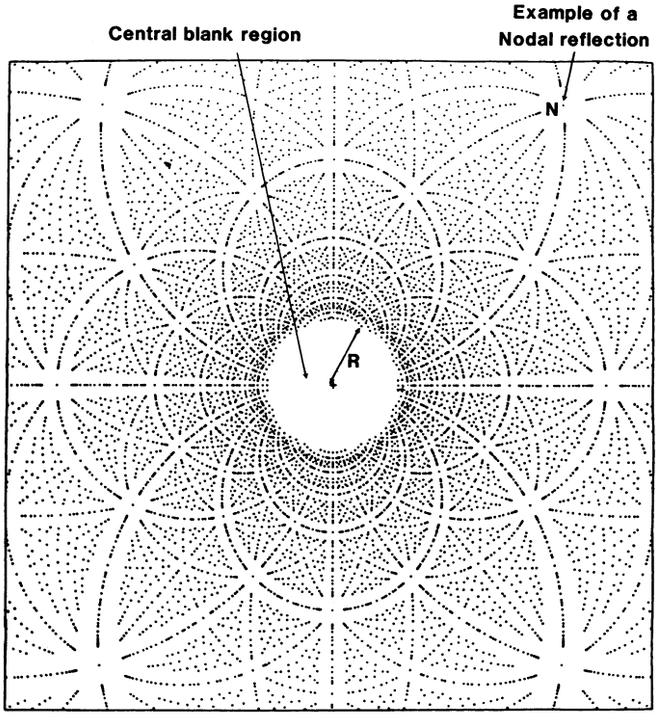

Fig. 2.2.1.2. A predicted Laue pattern of a protein crystal with a zone axis parallel to the incident, polychromatic X-ray beam. There is a pronounced blank region at the centre of the film (see Subsection 2.2.1.2). The spot marked *N* is one example of a nodal spot (see Subsection 2.2.1.4).

For a Laue spot at a given θ, only the ratio λ/d is determined, whether it is a single or a multiple relp component spot. If the unit-cell parameters are known from a monochromatic experiment, then a Laue spot at a given θ yields λ since d is then known. Conversely, precise unit-cell lengths cannot be determined from a Laue pattern alone; methods are, however, being developed to determine these (see Carr, Cruickshank & Harding, 1992).

The maximum Bragg angle θ_{max} is given by the equation

$$\theta_{max} = \sin^{-1}(\lambda_{max}/2d_{min}). \qquad (2.2.1.2)$$

2.2.1.2. *Crystal setting*

The main use of Laue photography has in the past been for adjustment of the crystal to a desired orientation. With small-molecule crystals, the number of diffraction spots on a monochromatic photograph from a stationary crystal is very small. With unfiltered, polychromatic radiation, many more spots are observed and so the Laue photograph serves to give a better idea of the crystal orientation and setting prior to precession photography. With protein crystals, the monochromatic still is used for this purpose before data collection *via* an area detector. This is because the number of diffraction spots is large on a monochromatic still and in a protein-crystal Laue photograph the stimulated spots from the *Bremsstrahlung* continuum are generally very weak. Synchrotron-radiation Laue photographs of protein crystals can be recorded with short exposure times. These patterns consist of a large number of diffraction spots.

Crystal setting *via* Laue photography usually involves trying to direct the X-ray beam along a zone axis. Angular mis-setting angles ε in the spindle and arc are easily calculated from the formula

$$\varepsilon = \tan^{-1}(\Delta/D), \qquad (2.2.1.3)$$

where Δ is the distance (resolved into vertical and horizontal) from the beam centre to the centre of a circle of spots defining a zone axis and D is the crystal-to-film distance.

After suitable angular correction to the sample orientation, the Laue photograph will show a pronounced blank region at the centre of the film (see Fig. 2.2.1.2). The radius of the blank region is determined by the minimum wavelength in the beam and the magnitude of the reciprocal-lattice spacing parallel to the X-ray beam (see Jeffery, 1958). For the case, for example, of the X-ray beam perpendicular to the a^*b^* plane, then

$$\lambda_{min} = c(1 - \cos 2\theta), \qquad (2.2.1.4a)$$

where

$$2\theta = \tan^{-1}(R/D) \qquad (2.2.1.4b)$$

and R is the radius of the blank region (see Fig. 2.2.1.2), and D is the crystal-to-flat-film distance. If λ_{min} is known then an approximate value of c, for example, can be estimated. The principal zone axes will give the largest radii for the central blank region.

2.2.1.3. *Single-order and multiple-order reflections*

In Laue geometry, several relp's can occur in a Laue spot or ray. The number of relp's in a given spot is called the multiplicity of the spot. The number of spots of a given multiplicity can be plotted as a histogram. This is known as the multiplicity distribution. The form of this distribution is dependent on the ratio $\lambda_{max}/\lambda_{min}$. The multiplicity distribution

in Laue diffraction is considered in detail by Cruickshank, Helliwell & Moffat (1987).

Any relp nh, nk, nl (n integer) will be stimulated by a wavelength λ/n since $d_{nhnknl} = d_{hkl}/n$, *i.e.*

$$\frac{\lambda}{n} = 2\frac{d_{hkl}}{n}\sin\theta. \qquad (2.2.1.5)$$

However, d_{nhnknl} must be $> d_{\min}$ as otherwise the reflection is beyond the sample resolution limit.

If h, k, l have no common integer divisor and if $2h$, $2k$, $2l$ is beyond the resolution limit, then the spot on the Laue diffraction photograph is a single-wavelength spot. The probability that h, k, l have no common integer divisor is

$$Q = \left[1-\frac{1}{2^3}\right]\left[1-\frac{1}{3^3}\right]\left[1-\frac{1}{5^3}\right]\ldots$$
$$= 0.832\ldots. \qquad (2.2.1.6)$$

Hence, for a relp where $d_{\min} < d_{hkl} < 2d_{\min}$ there is a very high probability (83.2%) that the Laue spot will be recorded as a single-wavelength spot. Since this region of reciprocal space corresponds to 87.5% (*i.e.* 7/8) of the volume of reciprocal space within the resolution sphere then $0.875 \times 0.832 = 72.8\%$ is the probability for a relp to be recorded in a single-wavelength spot. According to W. L. Bragg, all Laue spots should be multiple. He reasoned that for each h, k, l there will always be a $2h$, $2k$, $2l$ *etc*. lying within the same Laue spot. However, as the resolution limit is increased to accommodate this many more relp's are added, for which their hkl's have no common divisor.

The above discussion holds for infinite bandwidth. The effect of a more experimentally realistic bandwidth is to increase the proportion of single-wavelength spots.

The number of relp's within the resolution sphere is

$$\frac{4}{3}\frac{\pi d^{*3}_{\max}}{V^*}, \qquad (2.2.1.7)$$

where $d^*_{\max} = 1/d_{\min}$ and V^* is the reciprocal unit-cell volume.

The number of relp's within the wavelength band $\lambda_{\max}$ to $\lambda_{\min}$, for $\lambda_{\max} < 2/d^*_{\max}$, is (Moffat, Schildkamp, Bilderback & Volz, 1986)

$$\frac{\pi}{4}\frac{(\lambda_{\max}-\lambda_{\min})d^{*4}_{\max}}{V^*}. \qquad (2.2.1.8)$$

Note that the number of relp's stimulated in a 0.1 Å wavelength interval, for example between 0.1 and 0.2 Å, is the same as that between 1.1 and 1.2 Å, for example. A large number of relp's are stimulated at one orientation of the crystal sample.

The proportion of relp's within a sphere of small d^* (*i.e.* at low resolution) actually stimulated is small. In addition, the probability of them being single is zero in the infinite-band-width case and small in the finite-bandwidth case. However, Laue

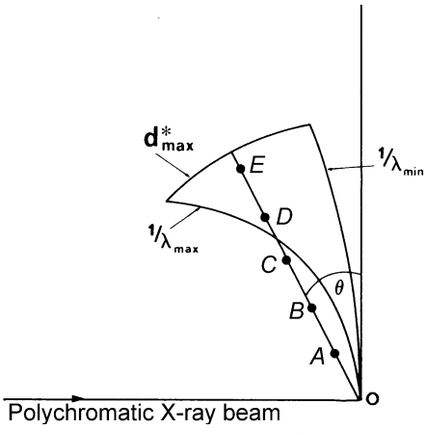

Fig. 2.2.1.3. A multiple component spot in Laue geometry. A ray of multiplicity 5 is shown as an example. The inner point A corresponds to d and a wavelength λ, the next point, B, is $d/2$ and wavelength $\lambda/2$. The outer point E corresponds to $d/5$ and $\lambda/5$. Rotation of the sample will either exclude inner points (at the $\lambda_{\max}$ surface) or outer points (at the $\lambda_{\min}$ surface) and so determine the recorded multiplicity.

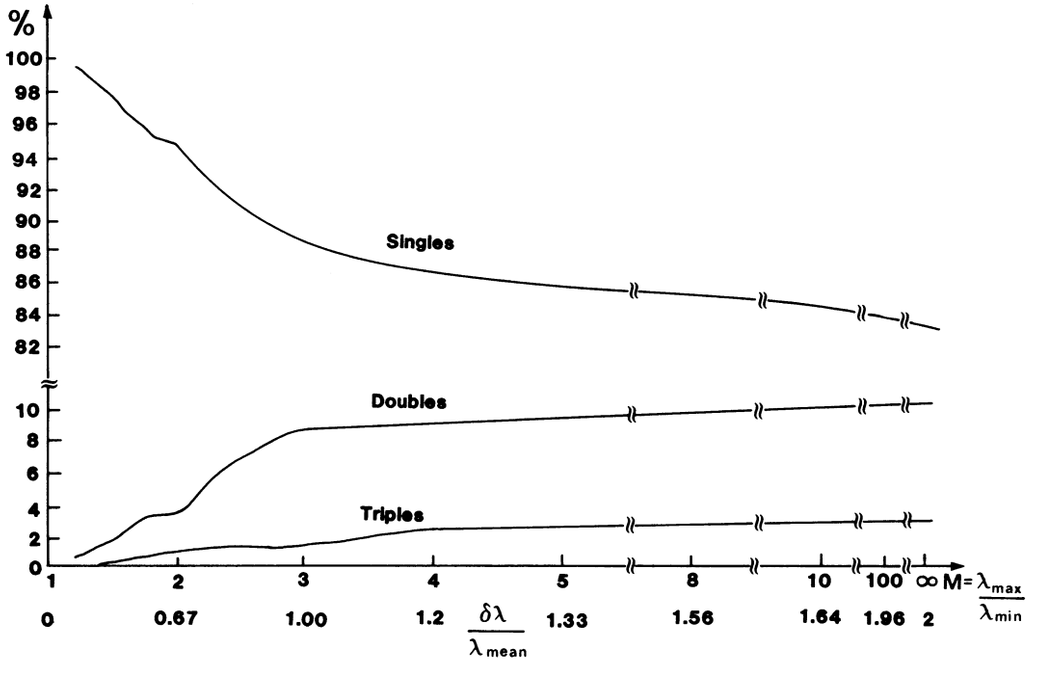

Fig. 2.2.1.4. The variation with $M = \lambda_{\max}/\lambda_{\min}$ of the proportions of relp's lying on single, double, and triple rays for the case $\lambda_{\max} < 2/d^*_{\max}$. From Cruickshank, Helliwell & Moffat (1987).

geometry is an efficient way of measuring a large number of relp's between d^*_{max} and $d^*_{max}/2$ as single-wavelength spots.

The above is a brief description of the overall multiplicity distribution. For a given relp, even of simple *hkl* values, lying on a ray of several relp's (multiples of *hkl*), a suitable choice of crystal orientation can yield a single-wavelength spot. Consider, for example, a spot of multiplicity 5. The outermost relp can be recorded at long wavelength with the inner relp's on the ray excluded since they need λ's greater than λ_{max} (Fig. 2.2.1.3). Alternatively, by rotating the sample, the innermost relp can be measured uniquely at short wavelength with the outer relp's excluded (they require λ's shorter than λ_{min}). Hence, in Laue geometry several orientations are needed to recover virtually all relp's as singles. The multiplicity distribution is shown in Fig. 2.2.1.4 as a function of $\lambda_{max}/\lambda_{min}$ (with the corresponding values of $\delta\lambda/\lambda_{mean}$).

2.2.1.4. *Angular distribution of reflections in Laue diffraction*

There is an interesting variation in the angular separations of Laue reflections that shows up in the spatial distributions of spots on a detector plane (Cruickshank, Helliwell & Moffat, 1991). There are two main aspects to this distribution, which are general and local. The general aspects refer to the diffraction pattern as a whole and the local aspects to reflections in a particular zone of diffraction spots.

The general features include the following. The spatial density of spots is everywhere proportional to $1/D^2$, where D is the crystal-to-detector distance, and to $1/V^*$, where V^* is the reciprocal-cell volume. There is also though a substantial variation in spatial density with diffraction angle θ; a prominent maximum occurs at

$$\theta_c = \sin^{-1}(\lambda_{min} d^*_{max}/2). \qquad (2.2.1.9)$$

Local aspects of these patterns particularly include the prominent conics on which Laue reflections lie. That is, the local spatial distribution is inherently one-dimensional in character. Between multiple reflections (nodals), there is always at least one single and therefore nodals have a larger angular separation from their nearest neighbours. The blank area around a nodal in a Laue pattern (Fig. 2.2.1.2) has been noted by Jeffery (1958). The smallest angular separations, and therefore spatially overlapped cases, are associated with single Laue reflections. Thus, the reflections involved in energy overlaps – the multiples – form a set largely distinct, except at short crystal-to-detector distances, from those involved in spatial overlaps, which are mostly singles (Helliwell, 1985).

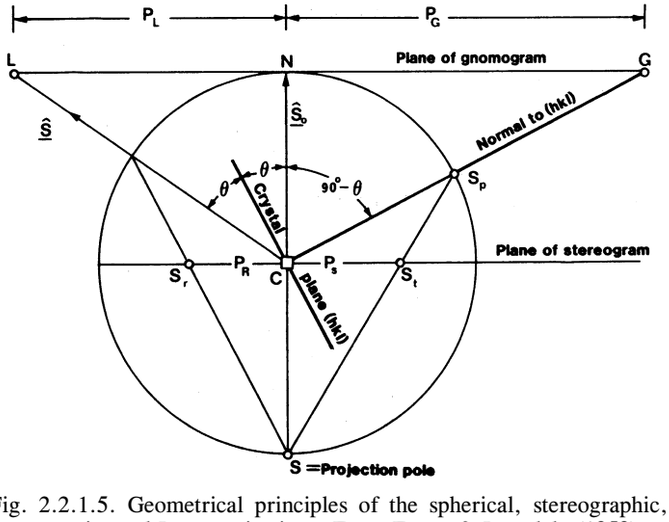

Fig. 2.2.1.5. Geometrical principles of the spherical, stereographic, gnomonic, and Laue projections. From Evans & Lonsdale (1959).

From a knowledge of the form of the angular distribution, it is possible, *e.g.* from the gaps bordering conics, to estimate d^*_{max} and λ_{min}. However, a development of this involving gnomonic projections can be even more effective (Cruickshank, Carr & Harding, 1992).

2.2.1.5. *Gnomonic and stereographic transformations*

A useful means of transformation of the flat-film Laue pattern is the gnomonic projection. This converts the pattern of spots lying on curved arcs to points lying on straight lines. The stereographic projection is also used. Fig. 2.2.1.5 shows the graphical relationships involved [taken from *International Tables*, Vol. II (Evans & Lonsdale, 1959)], for the case of a Laue pattern recorded on a plane film, between the incident-beam direction *SN*, which is perpendicular to a film plane and the Laue spot L and its spherical, stereographic, and gnomonic points S_p, S_t and G and the stereographic projection S_r of the reflected beams. If the radius of the sphere of projection is taken equal to D, the crystal-to-film distance, then the planes of the gnomonic projection and of the film coincide. The lines producing the various projection poles for any given crystal plane are coplanar with the incident and reflected beams. The transformation equations are

$$P_L = D\tan 2\theta \qquad (2.2.1.10)$$

$$P_G = D\cot\theta \qquad (2.2.1.11)$$

$$P_S = D\frac{\cos\theta}{(1+\sin\theta)} \qquad (2.2.1.12)$$

$$P_R = D\tan\theta. \qquad (2.2.1.13)$$

2.2.2. Monochromatic methods

In this section and those that follow, which deal with monochromatic methods, the convention is adopted that the Ewald sphere takes a radius of unity and the magnitude of the reciprocal-lattice vector is λ/d. This is not the convention used in the Laue section above.

Some historical remarks are useful first before progressing to discuss each monochromatic geometry in detail. The original rotation method (for example, see Bragg, 1949) involved a rotation of a perfectly aligned crystal of 360°. For reasons of relatively poor collimation of the X-ray beam, leading to spot-to-spot overlap, and background build-up, Bernal (1927) introduced the oscillation method whereby a repeated, limited, angular range was used to record one pattern and a whole series of contiguous ranges on different film exposures were collected to provide a large angular coverage overall. In a different solution to the same problem, Weissenberg (1924) utilized a layer-line screen to record only one layer line but allowed a full rotation of the crystal but now coupled to translation of the detector, thus avoiding spot-to-spot overlap. Again, several exposures were needed, involving one layer line collected on each exposure. The advent of synchrotron radiation with very high intensity allows small beam sizes at the sample to be practicable, thus simultaneously creating small diffraction spots and minimizing background scatter. The very fine collimation of the synchrotron beam keeps the diffraction-spot sizes small as they traverse their path to the detector plane.

references